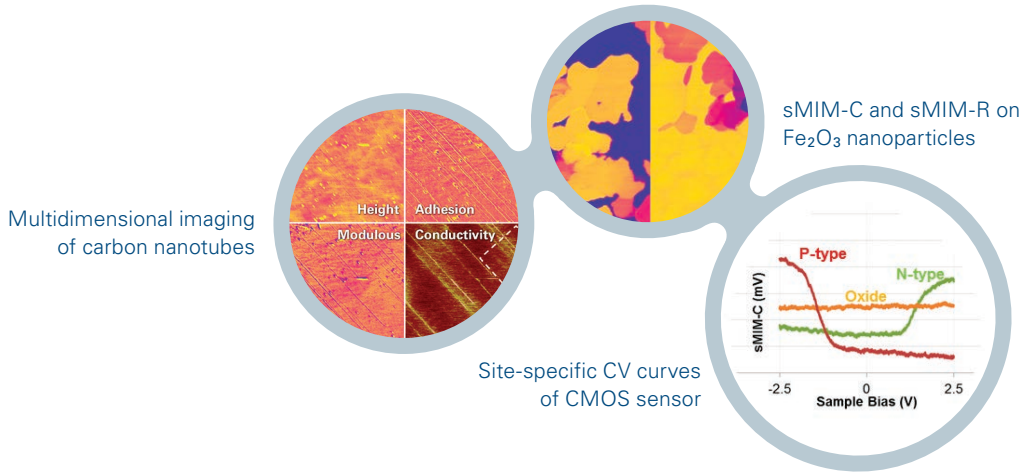

Application Note #145

Nanoscale Mapping of Permittivity and Conductivity with Scanning Microwave Impedance Microscopy

Scanning microwave impedance microscopy (sMIM) is an AFM-based technique for materials and device characterization. The reflected microwave signal from the tip-sample interface holds information of the electrodynamic properties of the sample surface underneath the tip apex. Detecting and processing of the reflectance in real time allows sMIM to directly access the permittivity and conductivity of materials. When an AFM-type sMIM probe is scanning across the sample surface, sMIM is capable of imaging variations in resistive (sMIM-R) and capacitive (sMIM-C) properties. This detection approach does not require making electrical contact between the sample and the substrate as sMIM is based on the capacitive coupling between the tip and the sample. By AC-biasing the sample or device under test, sMIM also provides carrier profiling (dC/dV) capability similar to traditional scanning capacitance microscopy (SCM). In the same way, it also uniquely offers mapping of nonlinear resistive properties (dR/dV). With both the sMIM and its AC-sample-bias modulated signals, sMIM is suitable for studying surfaces with complex composition or devices under test with a broad dynamic range, e.g., metallic, semiconducting, and insulating domains. As a near-field method, the resolution of sMIM is only limited by the tip radius of the probe, and it can easily achieve a lateral resolution of <30 nm for electrical mapping. Sub-aF sensitivity and high S/N ratios are realized by using waveguide tips with coaxial shielding. Having these unique capabilities, sMIM is superior to other AFM-based electrical modes for a broad range of applications. This application note provides an introduction of sMIM and its integration with Bruker's versatile AFM platforms, such as the Dimension Icon® and Dimension Edge™ AFMs. When combined with Bruker's exclusive PeakForce Tapping® mode, it is possible to obtain sMIM results on delicate samples, such as carbon nanotubes. PeakForce Tapping (with PeakForce QNM®) additionally provides simultaneous mapping of other sample properties, including modulus and adhesion.

Introduction

In materials research and device characterization, physical properties of a material are often revealed by measuring response from an electromagnetic excitation. In the far-field radiation region, the best spatial resolution for electrical properties that can be achieved is on the order of a half wavelength, known as the Abbe's diffraction barrier.[1] This far-field limit breaks down when using subwavelength aperture or apertureless waveguide techniques. This is the essence of near-field measurement and provides spatially resolving power defined by the spatial extent of the evanescent fields, rather than the free-space wavelength. In the microwave regime, the free-space wavelength is more than a millimeter, making it impossible to characterize materials on the nanoscale (less than one millionth of the

microwave wavelength). Near-field microscopy was first demonstrated at microwave frequencies in 1950s,[2] about 30 years after the original proposal by Synge.[3] Now, it has been extended to other spectral regions, such as far infrared, infrared, and visible regimes.[4]

In near-field microscopy, the probe is required to be very close to the sample surface as the evanescent or near-field contribution of the electromagnetic field decays exponentially with distance. In atomic force microscopy, metallic or metal-coated probes enable near-field measurements as they are suited for both near-field detection and atomic force microscopy imaging. This allows for serial pixel-to-pixel data acquisition where the spatial resolution is primarily determined by the dimension of the tip apex. These techniques are now commercially available. Examples include tip-enhanced Raman spectroscopy (e.g., Bruker's Innova-TERS) and scattering SNOM in the infrared domain (e.g., Bruker's Inspire).[5-8] For microwave frequencies, scanning microwave impedance microscopy (sMIM) is an important example, and is the focus of this application note.

In sMIM, the tip terminates the microwave transmission line. Its impedance is a function of the tip-to-sample coupling capacitance, the tip stray capacitance, and the tip-sample impedance.[9] When the tip-sample distance is much smaller than the characteristic tip size, and appropriate shielding is applied, the tip-sample impedance is dominated by the sample "near-field" impedance, which holds information about the electrical properties of the sample. The tip as an "open" end of the transmission line is an impedance discontinuity that results in the reflection of the microwave. The reflection coefficient is a function of the tip impedance, and thus, the sample "near-field" impedance. Therefore, by imaging the microwave reflectance, one can get access to the local electrical properties, e.g., permittivity and conductivity, of the material surfaces just beneath the tip.

Compared to other AFM-based electrical modes, sMIM has many advantages. First, it directly images the variation of permittivity and conductivity when the tip scans across sample surfaces. This allows for differentiation of materials with a wide dynamic range, from metals and semiconductors to insulators and dielectrics. Second, the measurement is based on tip-sample capacitive coupling (or microwave reflection). Therefore, sMIM does not require electrical contact between sample and substrate for mapping electrical properties, as is the case with conductive AFM or surface potential/Kelvin Probe force microscopy (KPFM). This is a critical concern on those samples where it is impossible to add an electrical contact or where electrical contact alters material properties. Graphene and MoS_2 are two typical examples, but in actuality, most of the nanoscale 2D materials fit this use case. Measuring islands, films, or particles on a non-conductive substrate or in an insulating material can also take advantage of this capability. In this sense, sMIM is a truly non-invasive method for nanoelectrical measurements. Third, by modulating the sample with an AC bias, the corresponding AC response of sMIM signals can be captured. For non-linear materials, such as semiconductor materials and devices, the AC-sMIM signal varies with doping density. Similar to traditional scanning capacitance microscopy (SCM),[10-11] this AC output has phase and amplitude signals that reflect the different types of dopants and variation of the doping density. Compared to SCM, sMIM can also provide capacitive and resistive channels, as well as the AC response of the resistive information. For failure analysis, local and site-specific capacitance-voltage and resistance-voltage spectroscopy also provides important information. In this way, sMIM has direct access to the permittivity and conductivity, which remains highly challenging for other methods, such as SCM. In addition, sMIM is based on microwave-matter interaction, where the electromagnetic field can penetrate a certain distance into the sample (exponential decay inside a medium). This makes electrical imaging of subsurface structures possible. The depth sensitivity depends on the spatial distribution of the near field inside the medium. These advantages allow one to apply the sMIM method for a broad range of materials, including biological samples, low-dimensional structures, polymers, ferroelectrics, composites, semiconductor devices, etc. This application note showcases examples that also leverage the unique capabilities of Bruker's AFM platforms.[12]

Performing sMIM with Bruker AFMs

The sMIM setup on a Bruker AFM features a probe holder that can accommodate regular AFM probes as well as dedicated, shielded AFM probes. For sMIM operation, the probe is part of the transmission line that carries the microwave to the tip-sample interface. Therefore, a conductive probe is inevitably required for electrical measurement. To account for noise level and minimal topographical convolution, probes with a coaxial shielding structure are highly recommended. This batch-fabricated, commercially-available, coaxially shielded probe is one of the critical factors that determines the ultra-high sensitivity, a factor of ten higher than traditional techniques. As shown in Figure 1, the probe has a center metal trace buried in insulating dielectric layers. It conducts the microwave signal between the electrode and metal tip. The metal layers on both sides of the cantilever form a coaxially shielded structure. This shielding dramatically eliminates stray and parasitic capacitance, and reduces other noises from the surrounding environment. It also ensures only the tip apex interacts with the sample during scanning. Together with the <50 nm radius, the coaxially shielded structure provides high electric sensitivity and spatial resolution. In addition, the use of a conductive probe on Bruker's versatile AFM platforms allows the integration of other electrical measurements with sMIM to provide simultaneous multimodal information, such as piezoelectricity and surface potential.[10-13]

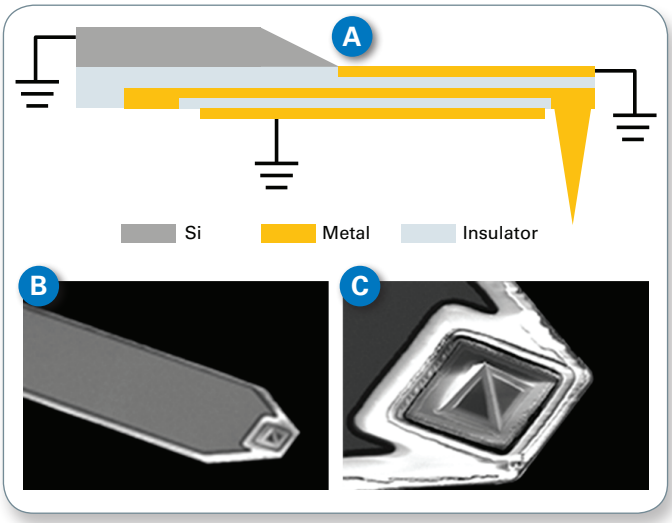

Figure 1. (A) Illustration of the coaxially shielded structure of the sMIM probe with a tip radius <50 nm. The metal layers on both sides of the cantilever form a coaxial shield to eliminate stray and parasitic capacitance, and reduce noise from the surrounding environment. The central metal line transmits the microwave to the tip apex. (B) and (C) are SEM images of a typical sMIM probe.

In a typical sMIM system, a matching network allows for the transmission of a low-power 3 GHz signal to the apex of the tip. This electronics output is set by default at -20 dBm and can be varied from -10 to -40 dBm. The optimal frequency often has a slight deviation (few to tens of MHz) from the 3 GHz due to the variation of individual probe characteristics, and is selected to minimize the reflectance (Γ) from the probe and probe interface assembly. When the tip is engaged and scanning across the sample surface, sMIM detects the reflected microwave signals due to a variation in the system impedance from Z_0:

$$\Gamma = \frac{Z_{tip} - Z_0}{Z_{tip} + Z_0}$$

The probe-sample impedance, Z_{tip}, can be expressed as a lumped element model as shown in Figure 2. The reflected signal from the tip-sample interface is coupled back into the circuit. An RF mixer resolves the in-phase (real) and the out-of-phase (imaginary) signals that are correlated with sample conductivity and permittivity, respectively. These two output signals are labeled as sMIM-R and sMIM-C. After adjustment of the demodulation phase on a reference sample, both the resistive (sMIM-R) and capacitive (sMIM-C) channels are isolated, imaged spatially, and displayed independently as images or "maps."

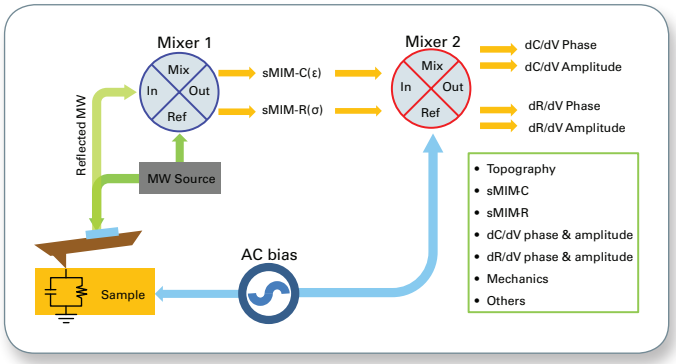

Figure 2. Schematic diagram of sMIM. The tip-sample impedance is described as a lumped element circuit model. The reflected microwave is resolved by an RF mixer (Mixer 1) into sMIM-C (capacitive) and sMIM-R (resistive) channels, which are related to permittivity and conductivity of the sample, respectively. When the sample is AC biased, the AC component of the sMIM signals are further resolved by lock-in amplifiers to provide dC/dV information for carrier profiling and dR/dV channels for other analysis.

When the sample is AC biased, the AC component of the sMIM signals are further resolved by lock-in amplifiers to provide the in-phase and out-of-phase signals. For the sMIM-C channel this corresponds to the dC/dV amplitude and phase signals (similar to SCM). In this way, sMIM is capable of carrier profiling (as SCM) while simultaneously also providing the low-frequency (3 GHz) dielectric contrast of the sample surface. This greatly expands sMIM's applications in semiconductor failure analysis as compared to SCM. In addition, sMIM provides the unique channel dR/dV, another layer of information for characterizing materials and devices. It also can be operated in contact mode or while the cantilever is oscillating.

With these sMIM capabilities in mind, Bruker's exclusive Peakforce Tapping mode is of high interest and brings a number of advantages. First, Peakforce Tapping enables simultaneous mapping of electrical properties with mechanical properties (adhesion, modulus, deformation, dissipation) through PeakForce QNM. Second, the precise, linear force control in PeakForce Tapping allows one to use extremely low imaging forces (routinely <100 pN), enabling the study of fragile and soft materials, or materials that are loosely attached to the substrate. For the same reason, tip lifetime—often a concern in electrical AFM modes—is drastically increased. When interleave mode is used, even more information (e.g., surface potential or piezoelectricity) can be captured simultaneously.[10-13] Correlating all this information with surface morphology provides true multi-dimensional nanoscale characterization. Thus, sMIM provides a very powerful tool kit for both materials characterization and device failure analysis. This application note is a collection of a variety of application examples for different application areas.

sMIM Case Studies

Static Random Access Memory (SRAM)

Front-side-polished SRAM samples have a variety of topographical features relating to implant regions. They are often used as a reference and test sample for SCM measurements to confirm basic capabilities to image doped samples and differentiate the carrier types and various doping levels on a device. While scanning in SCM mode, the tip and sample form a small capacitor. The capacitance varies with the depletion/accumulation depth modulated by an AC sample bias applied to the sample. SCM measures AC-modulated capacitance with change in applied AC sample bias, dC/dV. The dC/dV phase and amplitude are used to differentiate respectively dopant types and doping concentrations. Though sMIM has similar functionality, it further adds the capability of mapping dielectric properties.

Figure 3 presents an example of sMIM measurements on SRAM samples. Figure 3A shows the topography in 3D rendering. The area imaged is 15 µm x 7.5 µm using contact mode showing a flat substrate, ~100 nm tall rough region, and the ~150 nm height features. sMIM-C channel in Figure 3B shows permittivity variation across the sample surface. The edges on each 150 nm tall plateau have different permittivity compared to the plateau itself. The dC/dV phase image in Figure 3C resolves all the details of this "O" structure, such as epitaxial p-type substrate, n-type low-doped drain, p-type gate and n-type channels. On Figure 3D, the image of relative doping

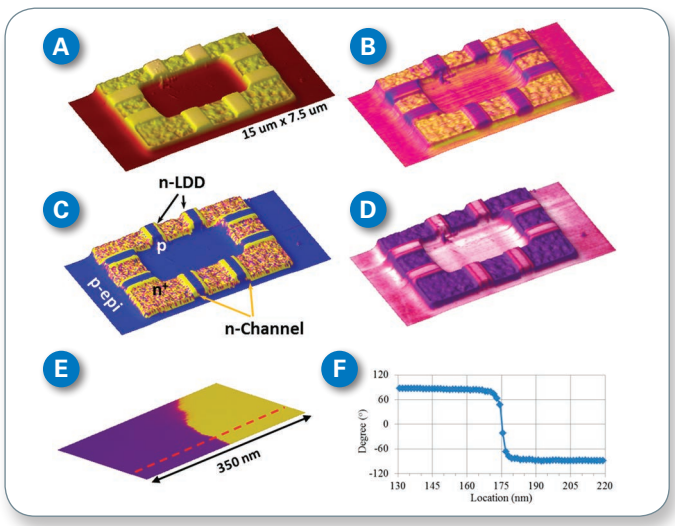

Figure 3. sMIM images of a SRAM samples. (A) Topography channel, 15 µm x 7.5 µm, and ~150 nm tall features; (B) sMIM-C channel as a skin covers on topography; (C) sMIM dC/dV phase channel on topography; (D) sMIM dC/dV amplitude channel on topography; (E) a topographically featureless (roughness < 0.1 nm) region with two clearly different doping regions; and (F) cross-sectional analysis of the phase transition as indicated by the red line on the image in (E).

density also shows the depletion layer when transitioning from p- to n-type, as indicated by the dark lines on the flat plateau. Figure 3E demonstrates the ability to achieve high- resolution electrical imaging on topographically featureless surfaces. The cross-sectional analysis of the phase image is plotted in Figure 3F showing a sharp transition, <10 nm, from p- to n-type doped regions.

Inverted Vertical Insulated Gate Bipolar Transistors (IGBTs)

IGBTs are one of the most important types of discrete power semiconductor devices. These devices were developed to combine high efficiency and fast switching. Characterizing the architecture at the nanoscale and understanding the doping level and carrier type at different locations in the device are critical to the design and performance of IGBT devices.

Figure 4 shows an example of microscopic studies on an IGBT cross-sectioned sample. SEM, as shown in Figure 4A, is widely used to reveal the different device components, such as metal contacts, gate oxide, poly-Si trench gate, and single crystal silicon (SC-Si) source and body. As sMIM-C images local dielectric variation, it also differentiates domains of single crystal Si with different doping densities. This is illustrated in Figure 4A by the clear emitter domains in the sMIM-C channel. The emitters connect directly to the tungsten contact strip. Both the ~125 nm tall tungsten contacts and the rough common emitter/source metal contacts can potentially pose challenges for imaging and tip-lifetime, and could also result in topographical convolution into the electrical data. This can be eliminated by integration of sMIM with PeakForce Tapping, as shown later in this application note. As demonstrated by this IGBT sample, sMIM has similar capabilities as SCM for carrier profiling. In Figure 4C and Figure 4D, the dC/dV amplitude and phase provide important information about the carrier concentration and carrier type, respectively. Based on the dC/dV phase and amplitude, one can construct an image simultaneously illustrating both the doping density and dopant types, similar to a traditional SCM image as shown in Figure 4D.

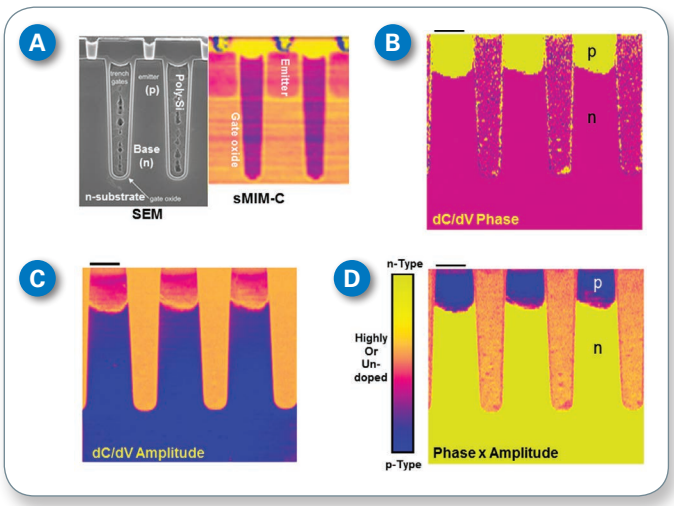

Figure 4. SEM and sMIM studies of an IGBT cross-section-polished sample from Chipworks. (A) Comparison of SEM and sMIM-C results on resolving different materials; (B) sMIM dC/dV phase image; (C) sMIM dC/dV amplitude channel; and (D) An image constructed from (B) and (C), similar to a traditional SCM image. Scale bar is1 µm. SEM image courtesy of Chipworks.

For failure analysis, traditional imaging methods such as SEM and SCM have distinct limitations in investigating the many features of certain devices, such as the IGBT shown here. SEM requires special, difficult-to-implement etching techniques to preferentially etch doping regions for sufficient contrast. Therefore, SCM is often used to resolve the different doping regions. However, SCM is only sensitive to nonlinear regions (i.e., doped semiconductor regions) and shows no contrast in metals, dielectrics, or regions with varying oxide thickness. In contrast, sMIM does not require any special sample prep to resolve the doped regions and can also differentiate oxide, semiconductor, and metals.

Complementary Metal-Oxide Semiconductor (CMOS) Image Sensors

In Figure 5, a front-side illuminated global-shutter CMOS image sensor was used to illustrate the high sensitivity of sMIM to a broad range of doping concentrations, as well as the contrast from such linear regions as shallow trench isolation, polysilicon, and dielectrics.[14] The sample features 3 µm pitch pixels. The sMIM-C channel in Figure 5B clearly resolves all key features, including (1) n-well storage diffusion; (2) n-well photocathode diffusion; (3) shallow trench isolation; (4) contact; and (5) p-type substrate surrounding cathode. The sMIM-R signal is captured simultaneously as well, as shown in Figure 5C. The sMIM-R response is weaker than the sMIM-C, likely due to the presence of the surface oxide, and because domains are either highly conductive or insulating. The sMIM-R signal is related to resistive loss and peaks at intermediate conductivity.

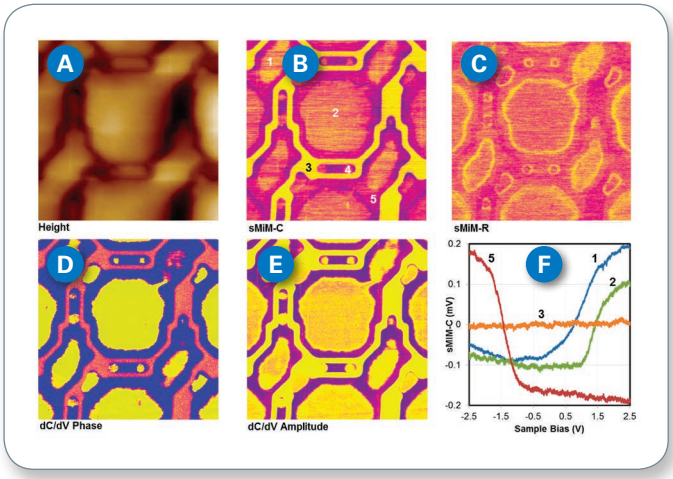

Figure 5. sMIM images of a front-side illuminated global-shutter CMOS image sensor from Chipworks.[14] The sample features 3 µm pitch pixels. (A) Topography; (B) sMIM-C; (C) sMIM-R; (D) dC/dV phase, solid yellow, 90° and solid blue, -90°; (E) dC/dV amplitude; and (F) site-specific capacitance-voltage curves at locations labelled in (B). The numbering in (B) features: (1) n-well storage diffusion; (2) n-well photocathode diffusion; (3) shallow trench isolation; (4) contact; and (5) p-type substrate surrounding cathode. The sMIM-C channel illustrates success in differentiating materials with a large dynamic range: metallic, semiconducting, and insulating. Scan size is 5 µm x 5 µm. For color code from (B) to (E), the yellower indicates the lower value. (B) and (C) have the sample scale bar in color contrast (-30 mV to 30 mV). These images were captured with a Dimension Edge AFM at Chipworks.

The dC/dV phase in Figure 5D appears as expected and similar to standard SCM imaging. N-type regions (solid yellow, 90°) and p-type regions (solid blue, -90°) are differentiated, whereas all other areas appear with a phase signal around 0°. The dC/dV amplitude (Figure 5E) features different doping densities for non-linear material, such as Si in this sample, with the dopant sensitivity ranging from 10^{14} cm^{-3} to 10^{20} cm^{-3} for sMIM. Though the dC/dV amplitude channel looks similar to the sMIM-C, the sMIM-C channel demonstrates a larger dynamic range. For example, comparing locations #3 (oxide) and #4 (highly doped Si) in the sMIM-C channel with the dC/dV amplitude channel, the SMIM-C signal in #3 is different from #4, whereas dC/dV amplitude shows almost no contrast between #3 and #4. The difference in signal is a result of dC/dV amplitude being peaked at intermediate dopant values while the sMIM-C signal is monotonic with dopant concentration.

The sMIM technique is also able to perform capacitance-voltage (C-V) spectroscopy by using the sMIM-C signal. Site-specific C-V spectroscopy can be used as a failure analysis tool for semiconductor devices. As shown in Figure 5F, plot #1 and #2 confirm n-type regions (n-well storage diffusion and n-well photocathode diffusion), while plot #5 demonstrates the p-type substrate surrounding the cathode. Plot #3 is corresponding to the oxide of shallow trench isolation.

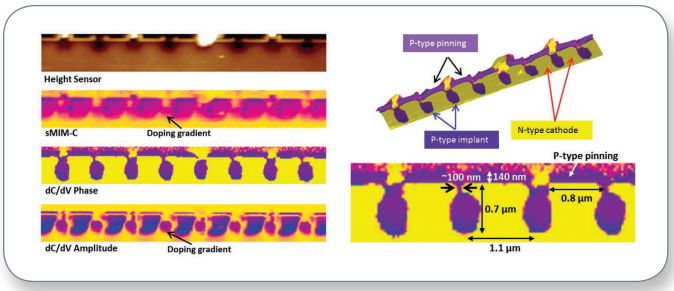

Figure 6. sMIM images of a Samsung S5K2P2XX CMOS image sensor from Chipworks. This sensor has 1.1 µm pixel features. SEM imaging is challenging to differentiate different implant regions. Only under certain etching conditions will the SEM image display some n- and p-type contrast.

To further demonstrate sMIM's ability in gaining a nuanced view of the device structure beyond the doping and carrier type information, Figure 6 shows another example on another type of CMOS image sensor device. This sensor has 1.1 µm pixel features. The important features can be characterized in detail by sMIM. First, the doping gradient of the photosensitive p-doped region is crucial to the device. Both the sMIM-C and dC/dV amplitude images provide high sensitivity to small dopant variations. Second, sMIM dC/dV phase clearly shows the doping carrier types with high contrast. Third, the pinning layer is resolved with detail allowing for direct measurement of the layer thickness (~140 nm) and spacing (0.8 µm).

Semiconductor Metal Oxide Films

Iron oxide nanoparticles, in different phases, are widely used for a variety of practical applications, including photovoltaics,[15] solar-fuels generators,[16] storage devices, and bio sensors.[17-18] Their electrical properties greatly impact device performance. Again sMIM is a powerful tool for characterizing nanoparticle materials. Figure 7A shows a γ-Fe_2O_3 nanoparticle film used in recording media. Spindle-like particles with 100 nm x 500 nm size were deposited into a continuous film. This sample has conductivity inhomogeneity across the surface and has been used as a reference sample in conductive AFM modes. The local impedance of the sample varies across the sample surface and also shows contrast on both the sMIM-C and sMIM-R channels as shown in Figure 7.

This sample nicely illustrates that sMIM can be applied not only for semiconductor devices but also to many other materials systems. On this γ-Fe_2O_3 film, iron oxides with the rich oxygen vacancies are generally believed to be n-type semiconductor materials. This has been proven by many bulk measurements. However, the sMIM dC/dV phase signals in Figure 7D show phase contact with 180° difference, indicating different dopant types for different nanoparticles across the film at the nanoscale.

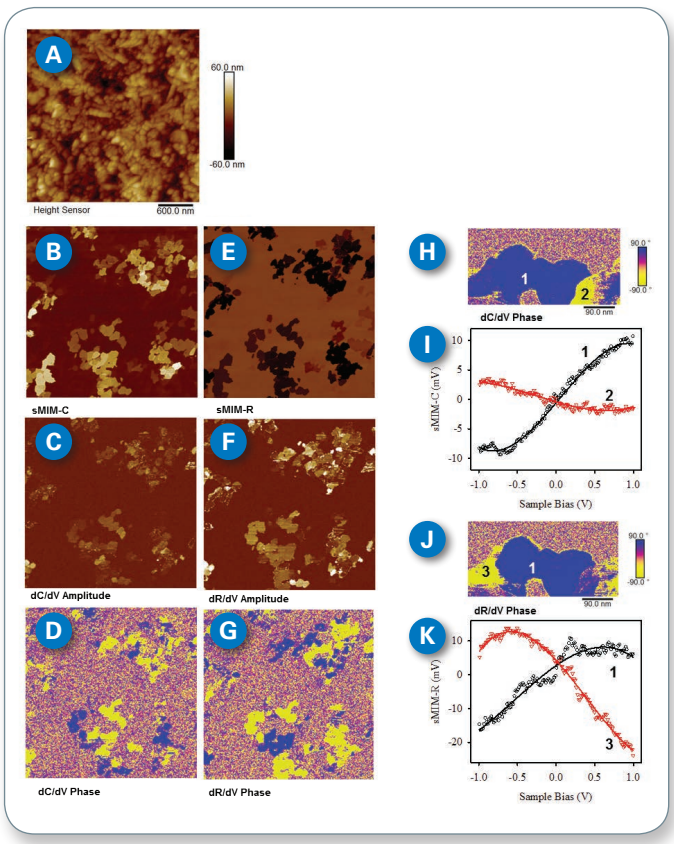

Figure 7. sMIM images and local capacitance-/resistance-voltage spectroscopy of a γ-Fe2O3 nanoparticle sample. (A) Topography shows 100 nm x 500 nm spindle particles; (B) sMIM-C reveals the location permittivity variation; (C) dC/dV amplitude; (D) dC/dV phase indicates different dopant polarities; (E) sMIM-R demonstrates different local conductivities; (F) dR/dV amplitude; (D) dR/dV phase; (H) high-resolution dC/dV phase image; (I) site-specific capacitance-voltage spectroscopy. Locations are indicated in (H); (J) high-resolution dR/dV phase image at the same location as (H); (K) site-specific resistance-voltage spectroscopy.

More interestingly, sMIM dR/dV amplitude and phase signals, as shown in Figure 7F and Figure 7G, also show clearly the amplitude contrast and domains with 180° phase differences. This further confirms that this oxide is a non-linear material. In addition, a comparison of dR/dV with dC/dV images shows distinct variations from each other. In the phase images, the contrast responses are clearly highlighting different aspects of the grains, and even within a specific grain (see Figure 7H and Figure 7J).

As shown in Figure 7I, C-V curves were captured from two distinct phase domains indicated in Figure 7H, which expects opposite signs of the slopes for these two curves. In addition, the slopes also indicate higher doping concentration on location #1 than #2. This greatly extends the understanding of the physics of this material.

Similarly, we also performed voltage-dependent sMIM-R sweeps at locations shown in Figure 7J, and the resulting R-V curves are shown in Figure 7K. Figure 7K further confirms inhomogeneous non-linear conductivity across the sample surface. This should be a concern for device design as applying an external voltage changes the conductivity of the samples at the nanoscale.

Buried Structures

The sMIM technique is based on electromagnetic interaction between microwave and matter. The concentrated electromagnetic field can penetrate into dielectric materials while decaying exponentially, which is a feature of evanescent or near field interaction. This long-range microwave-matter interaction is particularly useful for imaging buried structures. Figure 8 demonstrates the subsurface imaging ability of sMIM on a flat sample with dielectric variations resulting from the buried structures. The sample contains a patterned SiO_2 structure buried 133 nm under a Si_3N_4 film as shown in Figure 8A. The surface was polished to eliminate any residual topographic features. A surface roughness of 0.4 nm is achieved and shown in Figure 8B. Because of the permittivity difference between the oxide (ε = 3.9) and the nitride (ε = 7.5), the sMIM-C channel in Figure 8C clearly shows a response from the oxide patterns buried under the nitride. Where there is an oxide feature, the sMIM measures a lower capacitance than where there is no feature. While as expected, the oxide and nitride are both insulating, there is no variation in conductivity over the sample and the sMIM-R channel in Figure 8D shows no contrast.

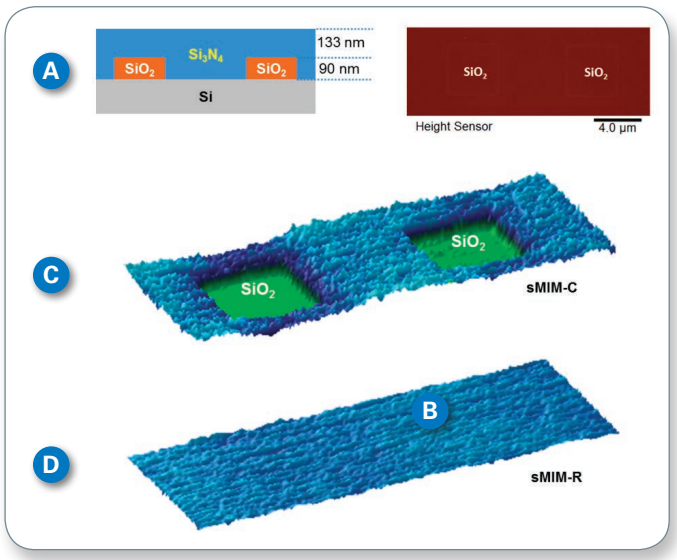

Figure 8. (A) A buried structure reference sample was fabricated on a Si wafer. 90 nm thermal SiO2 was grown on the wafer and patterned. 1um LPCVD Si3N4 was deposited to fully cover the SiO2. Chemical mechanical polishing was used to polish the sample until the Si3N4 was about 223 nm; (B) The topography of the polished reference surface with a roughness of 0.44 nm in the imaged area. (C) and (D) are sMIM-C and sMIM-R channels respectively. As expected, contrast only appears in the dielectric channel (sMIM-C) and vanishes in the conductivity channel (sMIM-R).

PeakForce Imaging and sMIM

In PeakForce Tapping, the probe and sample are intermittently brought into contact while the tip is scanning across the sample surface. The tapping frequency (1~2 kHz) is significantly lower than the cantilever's resonance (>10 kHz). This intermittent contact mechanism eliminates lateral forces during imaging and greatly prevents tip and sample damages from shear force. The feedback loop controls the maximum force, or peak force, on the tip, for each individual tapping cycle. With the sinusoidal, low-frequency, off-resonance mechanical modulation, the control algorithm is able to directly respond to the tip-sample force interaction. Unlike traditional linear ramping with a triangular wave (as used in Force Volume), the sinusoidal ramping in PeakForce Tapping allows the tip to approach the sample surface with a near-zero speed. This renders direct and stable force control so that the peak force can be routinely below 100 pN or even <50 pN. With this well-controlled gentle force and a 1~2 kHz tapping frequency, PeakForce Tapping not only protects the tip and the sample from damage but also offers high-resolution imaging while maintaining normal imaging rates. In addition, for every tapping cycle by the tip movement in the Z direction, PeakForce Tapping can acquire a force curve, enabling simultaneous imaging of quantitative mechanical properties directly correlated to topographic information.[19-20]

Similar to our other well-known PeakForce-enabled electrical modes—PeakForce TUNA™, PeakForce SSRM™ and PeakForce KPFM™—sMIM can also be integrated with PeakForce Tapping: PeakForce sMIM. It is important to note that the oscillation frequency (1 kHz to 2 kHz) of PeakForce Tapping results in a contact time of a few tens to hundreds of microseconds. This contact time is sufficiently long to collect the sMIM signals. sMIM can be performed to directly capture the cycle-averaged sMIM signals or with a sensor circuit similar to PeakForce TUNA to capture signals with a greatly improved signal-to-noise ratio. Alternatively, interleave mode can also be employed, similar to the PeakForce KPFM mode. In interleave mode, dark lift scanning with the AFM laser off in the lift scan can be very useful for characterizing light-sensitive materials.

PeakForce sMIM for Carbon Nanotubes

Figure 9 shows an example of PeakForce sMIM imaging of aligned carbon nanotubes (CNTs) that loosely attach to the substrate. Though this sample is challenging for contact mode, it can be imaged easily in PeakForce Tapping mode. Figure 9A is the topography channel showing the aligned CNTs on the insulating substrate. The mechanical channels (adhesion and modulus) in Figure 9B and Figure 9C, respectively, can better resolve the CNTs as they are highly sensitive to local mechanical properties. Different CNTs can have different conductivities, as confirmed by the sMIM-R channel. When comparing the black box in Figure 9B with the white box in Figure 9D, it is clear that these

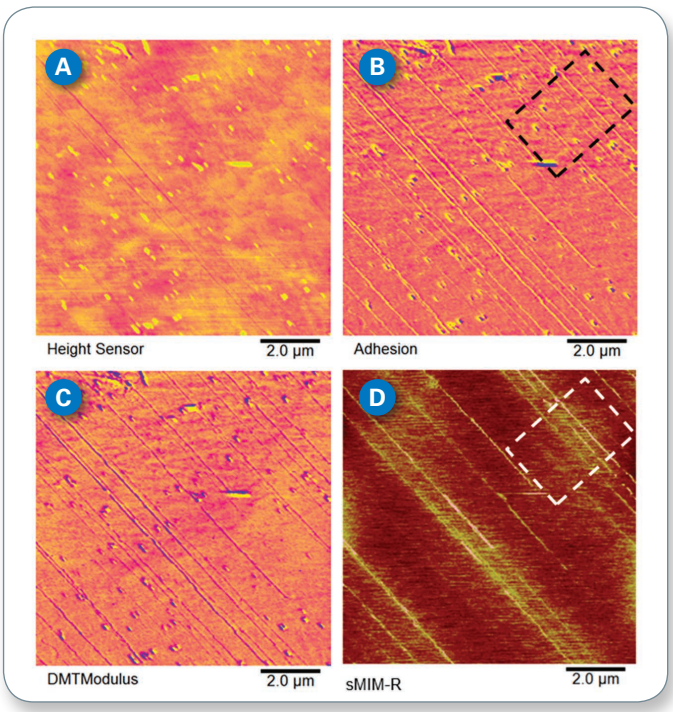

Figure 9. PeakForce sMIM images. (A) Topography; (B) adhesion; (C) DMTModulus; and (D) sMIM-R maps of carbon nanotubes (CNTs) aligned flat on an insulating substrate. Mechanical channels have higher sensitivity on visualizing the CNTs compared to topography. The sMIM-R channel confirms these CNTs have different conductivities as indicated by the square boxes on adhesion and sMIM-R channels. Note that no electrical contact is required as sMIM is performed based on tip-sample capacitive coupling.
Sample courtesy Greg Michael Pitner and Professor H.–S. Philip Wong, Stanford University.

CNTs have a similar adhesion but different conductivity. In addition, all the surface debris particles are gone in the sMIM-R channels as they have a similar sMIM-R response as the substrate. Importantly, there was no electrical contact made for this measurement. The sMIM imaging is based on capturing the reflected microwave from the impedance discontinuity (the tip-sample interface in this case) in the transmission line. Therefore, electrical contact is not required unless AC-biased modulation on the sample is needed for carrier profiling. This offers tremendous advantages for studying micro- and nano-size fragile materials where making electrical contact is extremely challenging or where electrical contact can alter the sample properties.

PeakForce sMIM for IGBTs

As mentioned above, for failure analysis, IGBT devices are often characterized by SEM for material structure. Similar to contact mode sMIM, as shown in Figure 10, the sMIM-C channel from PeakForce sMIM clearly shows such features as the dielectric gate oxide layer, the metallic gate contact, and the semiconducting emitter region. The emitter region is challenging to SEM and is not shown on the SEM image. More importantly, the use of PeakForce Tapping makes it easy to scan on the rough metal contact region, which is not trivial for contact mode. Imaging this region in contact mode easily wears the tip and reduces the image resolution. These issues can be well addressed by using PeakForce sMIM. As shown in Figure 10, for example, clear topographic and electrical features with more nuanced details can be seen in both the rough metal and semiconductor regions. The same probe was used for more than 10 images without performance degradation.

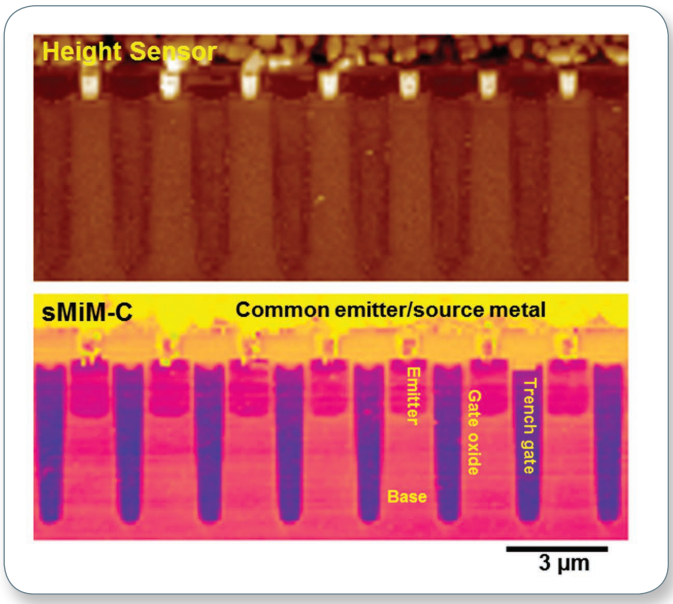

Figure 10. PeakForce sMIM imaging of an IGBT device. Compared to contact mode sMIM in Figure 4, clear topographic and electrical features with more nuanced details can be seen in both the rough metal and semiconductor regions. Additionally, the tip lifetime is greatly improved.

PeakForce sMIM for SRAM

Peakforce sMIM can also do carrier profiling, which combines the advantages from both PeakForce Tapping and sMIM in a single technique. Figure 11 is an example on an SRAM sample where different electrical channels are used as color skins on the 3D topographic views. The sMIM-C skin in Figure 11A is from raw data with no image post processing applied. This image shows minimal influences from the stray capacitance, which confirms the high performance of PeakForce sMIM. Figure 11B is the dC/dV phase, and Figure 11C is the dC/dV amplitude. All three images clearly show different electronic regions of the device, as labeled in Figure 11A. Compared to regular sMIM, these images have improved lateral resolution and overall sharpness. In addition, sMIM-C and dC/dV amplitude images show potential mask defects in the epitaxial p-type region where the doping concentration has a local variation near the two n-channels, as indicated by the highlighted area (black dotted line) in Figure 11C.

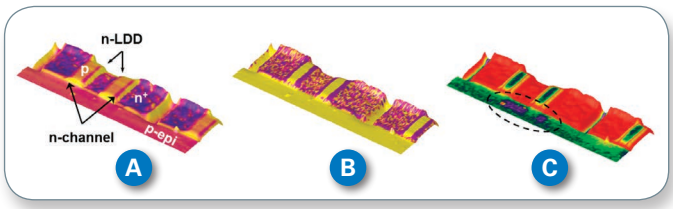

Figure 11. PeakForce sMIM images of an SRAM sample. Scan size is 12 µm x 4 µm. (A) sMIM-C channel as a skin covers on topography; (B) sMIM dC/dV phase channel on topography; (C) sMIM dC/dV amplitude channel on topography.

Conclusion

In summary, sMIM is a promising technique for charactering material electrical properties, such as permittivity and conductivity. Integrated with the precise topographic imaging capabilities of atomic force microscopy, the function of materials and devices can be probed with <20 nm resolution, adding new dimensions of information that directly correlate to the topographic channel. Importantly, this type of measurement of material electrodynamic properties does not require electrical contact with the substrate. This frees researchers and engineers from the tedious work of wiring and soldering that might alter the sample electrical properties and be impossible for nanoscale materials. Leveraging Bruker's versatile AFM platforms, not only can the capacitive and resistive properties be imaged, but the AC components resulting from the modulation of sample bias are scanned and resolved for dC/dV-type semiconductor carrier profiling and also add unique information from the dR/dV analysis. In addition, site-specific capacitance-voltage and resistance-voltage spectroscopy adds new tools for device failure analysis and for fundamental studies of novel materials. Finally, when empowered by Bruker's unique PeakForce Tapping, sMIM greatly expands its applications to previously challenging measurements on fragile samples

and also provides simultaneous mapping of correlated mechanical properties. The ability to directly image the local variation of a sample at the tens of nanometer length scales of sMIM has stimulated new areas of research and applications. CNTs, nanoparticle oxide films, subsurface patterns, and a variety of semiconductor devices discussed in this application note are just some of the examples. The versatility of sMIM leveraging Bruker's advanced AFM platforms will empower material researchers and device engineers to explore basic principles underlying functionality and perform more advanced and complete materials characterization and device failure analysis.

Table 1: sMIM Key Features / Specifications

Channels	sMIM-C sMIM-R
AC channels	dC/dV Phase dC/dV Amplitude dR/dV Phase dR/dV Amplitude
Scanning methods	Contact Tapping PeakForce Tapping Lift and Darklift
Probes	Shielded, metal tip, k=1 to 8 N/m
Frequency	3 GHz
Minimum detectable capacitance	0.5 aF
Dopant sensitivity range	10^{14} to 10^{20} atoms/cm^3
Spatial resolution (electrical)	<20 nm
Power	-15 dBm to -45 dBm
Instruments	Dimension Edge Dimension Icon Dimension Icon-GB

References

1. E. Abbe and F. Crisp, ed.,"On the Estimation of Aperture in the Microscope," *Journal of the Royal Microscopical Society* 1 (1881) 388.
2. Z. Frait, "The Use of High-Frequency Modulation in Studying Ferromagnetic Resonance," *Czechoslovak Journal of Physics* 9 (1959) 403.
3. E.H. Synge, "A Suggested Method for Extending Microscopic Resolution into the Ultra-Microscopic Region," *Philosophical Magazine* 6 (1928) 356.
4. B.T. Rosner and D.W. van der Weide, "High-Frequency Near-Field Microscopy," *Review of Scientific Instruments* 73 (2002) 2505.
5. S. Kaemmer, "AFM and Raman Spectroscopy — Correlated Imaging and Tip Enhanced Raman Scattering," Bruker Application Note #139 (2013).
6. S. Kaemmer, "Advances in Combined Atomic Force and Raman Microscopy," Bruker Application Note #136 (2012).
7. M. Wagner, "10nm-Resolution Infrared Chemical Mapping — Breaking the Diffraction Limit with Inspire" Bruker Application Note #143 (2015).
8. K.M.M. Carneiro, H. Zhai, L. Zhu, J.A. Horst, M. Sitlin, M. Nguyen, M. Wagner, C. Simpliciano, M. Milder, C.-L. Chen, P. Ashby, J. Bonde, W. Li, and S. Habelitz, "Amyloid-like Ribbons of Amelogenin in Enamel Mineralization," Scientific Reports, (2016 accepted).
9. S.M. Anlage, V.V. Talanov, and A.R. Schwartz, "Principles of Near-Field Microwave Microscopy," *Scanning Probe Microscopy*, Springer (2007).
10. "Electrical Characterization with Scanning Probe Microscopes," Bruker Application Note #079 (2008).
11. P. De Wolf, E. Brazel, and A. Erickson, "Electrical Characterization of Semiconductor Materials and Devices Using Scanning Probe Microscopy," *Materials Science in Semiconductor Processing* 4 (2001) 71.
12. S. Kaemmer, "Introduction to Bruker's ScanAsyst and PeakForce Tapping AFM Technology," Bruker Application Note #133 (2011).
13. C. Li, S. Minne, Y. Hu, J. Ma, J. He, H. Mittel, V. Kelly, N. Erina, S. Guo, and T. Mueller, "PeakForce Kelvin Probe Force Microscopy," Bruker Application Note #140: (2013).
14. B. Drevniok, St.J. Dixon-Warren, O. Amster, S.L. Friedman, and Y. Yang, "Extending Electrical Scanning Probe Microscopy Measurements of Semiconductor Devices Using Microwave Impedance Microscopy," ISTFA 2015: Conference Proceedings from the 41st International Symposium for Testing and Failure Analysis (2015) 77.
15. B.M. Klahr, A.B.F. Martinson, and T.W. Hamann, "Photoelectrochemical Investigation of Ultrathin Film Iron Oxide Solar Cells Prepared by Atomic Layer Deposition" *Langmuir* 27 (2011) 461.
16. C.W. Wang, S. Yang, W.Q. Fang, P. Liu, H. Zhao, and H.G. Yang, "Engineered Hematite Mesoporous Single Crystals Drive Drastic Enhancement in Solar Water Splitting" *Nano Letters* 16 (2016) 427.
17. G. Cordova, S. Attwood, R. Gaikwad, F. Gu, and Z. Leonenko, "Magnetic Force Microscopy Characterization of Superparamagnetic Iron Oxide Nanoparticles (SPIONs)," *Nano Biomedicine and Engineering* 6 (2014) 31.

18. S. Laurent, D. Forge, M. Port, A. Roch, C. Robic, L.V. Elst, and R.N. Muller, "Magnetic Iron Oxide Nanoparticles: Synthesis, Stabilization, Vectorization, Physicochemical Characterizations, and Biological Applications," *Chemical Reviews* 108 (2008) 2064.

19. A. Slade and S. Hu, "Imaging of the DNA Double Helix with PeakForce Tapping Mode Atomic Force Microscopy," Bruker Application Note #142 (2015).

20. J.H. Kindt, N. Phan, B. Pittenger, A. Mednick, A. Slade, L. Huang, W. Wang, N. Erina, J.E. Shaw, and S.C. Minne, "Survey, Screening, Dynamics: A No-Compromise Approach to High-Speed Atomic Force Microscopy" Bruker Application Note #134 (2013).

Authors

Zhuangqun Huang,[1] Benedict Drevniok,[2] Peter De Wolf,[1] St.John Dixon-Warren[2] Oskar Amster,[3] Stuart Friedman,[3] Bede Pittenger,[1] Chunzeng Li,[1] and Yongliang Yang[3]

[1] Bruker Nano Surfaces, Santa Barbara, CA 93117, USA
[2] Chipworks Inc, Ottawa, Ontario, K2H 5B7, Canada
[3] Prime Nano Inc., Palo Alto, CA 94306, USA

©2016 Bruker Corporation. All rights reserved. AN145, Rev. A0

Bruker Nano Surfaces Division
Santa Barbara, CA · USA
+1.805.967.1400
productinfo@bruker.com

www.bruker.com/afm